



Supplement of

Drivers of intermodel uncertainty in land carbon sink projections

Ryan S. Padrón et al.

Correspondence to: Ryan S. Padrón (ryan.padron@env.ethz.ch)

The copyright of individual parts of the supplement might differ from the article licence.

Model	SSP126	1pctCO2-bgc	Land surface model	Fire	Dynamic vegetation	Nitrogen cycle
ACCESS-ESM1-5	30	1	CABLE2.4 with CASA-CNP	No	No	Yes (and phosphorus)
CanESM5	50	1	CLASS-CTEM	No	No	No
CESM2	5	1	CLM5	Yes	No	Yes
CMCC-ESM2	1	1	CLM4.5	Yes	No	Yes
CNRM-ESM2-1	5	4	ISBA-CTrip	Yes	No	Implicit
EC-Earth3-Veg	5	1	HTESSEL and LPJ- GUESS	Yes	Yes	Yes
GFDL-ESM4	1	1	LM4.1	Yes	Yes	No
IPSL-CM6A-LR	6	1	ORCHIDEE, branch 2.0	No	No	No
MPI-ESM1-2-LR	10	3	JSBACH3.2	Yes	Yes	Yes
NorESM2-LM	1	0	CLM5	Yes	No	Yes
UKESM1-0-LL	16	1	JULES-ES-1.0	No	Yes	Yes

Table S1: Information on the Earth system models employed in the analysis. The columns SSP126 and 1pctCO2-bgc indicate the number of realizations from each model per scenario. The main analysis focuses on the shared socio-economic pathway SSP126, whereas the 1pctCO2-bgc simulations are used to estimate the sensitivity of GPP to CO₂ concentration (sCO₂).

5

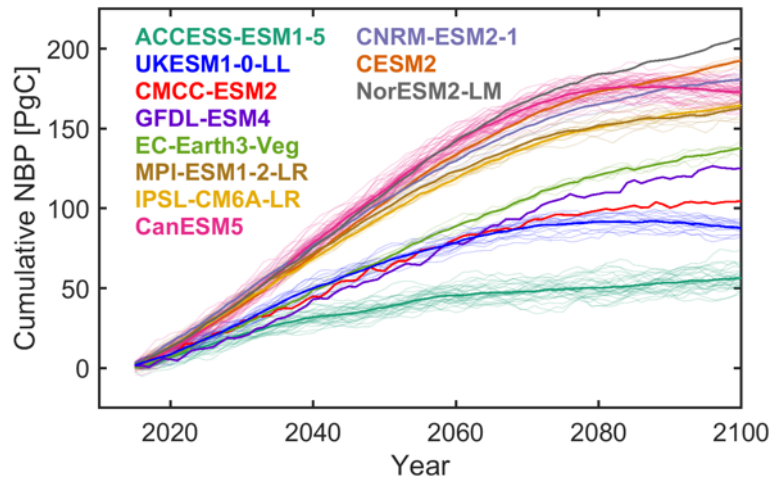
Model	Depth of the boundaries between soil moisture layers [m]
ACCESS-ESM1-5	0, 0.022, 0.08, 0.234, 0.643, 1.728, 4.6
CESM2	0, 0.025, 0.065, 0.125, 0.21, 0.33, 0.49, 0.69, 0.93, 1.21, 1.53, 1.89, 2.29, 2.745, 3.285, 3.925, 4.665, 5.505, 6.445, 7.485, 8.575
CMCC-ESM2	0, 0.0175, 0.0451, 0.0906, 0.1655, 0.2891, 0.4929, 0.8289, 1.3828, 2.2961, 3.8019, 6.2845, 10.3775, 17.1259, 28.2520, 42.1032
CNRM-ESM2-1	0, 0.01, 0.04, 0.1, 0.2, 0.4, 0.6, 0.8, 1, 1.5, 2, 3, 5, ,8, 12
CanESM5	0, 0.1, 0.35, 4.1
EC-Earth3-Veg	0, 0.07, 0.28, 1, 2.89
GFDL-ESM4	0, 0.02, 0.06, 0.1, 0.15, 0.2, 0.3, 0.4, 0.6, 0.8, 1, 1.4, 1.8, 2.2, 2.6, 3, 4, 5, 6, 7.5, 10
IPSL-CM6A-LR	0, 0.001, 0.004, 0.01, 0.022, 0.045, 0.092, 0.186, 0.374, 0.75, 1.5, 2
MPI-ESM1-2-LR	0, 0.065, 0.319, 1.232, 4.134, 9.834
NorESM2-LM	0, 0.025, 0.065, 0.125, 0.21, 0.33, 0.49, 0.69, 0.93, 1.21, 1.53, 1.89, 2.29, 2.745, 3.285, 3.925, 4.665, 5.505, 6.445, 7.485, 8.575
UKESM1-0-LL	0, 0.1, 0.35, 1, 3

Table S2: Soil layer discretization of employed Earth system models.

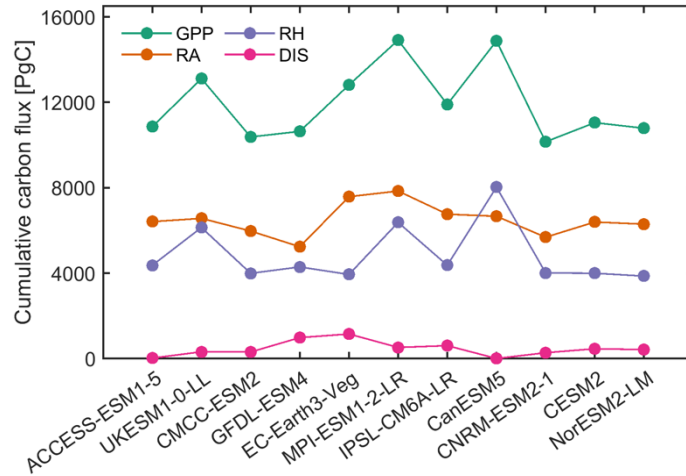
Model	Global						Tropics					
	NBP _{anom}	sCO ₂	sT	sSM	T	SM	NBP _{anom}	sCO ₂	sT	sSM	T	SM
ACCESS-ESM1-5	-7.27	-2.86	-3.73	1.24	-1.44	-0.48	-12.63	-2.55	-8.25	2.45	-3.69	-0.60
UKESM1-0-LL	-3.54	-0.20	-1.80	-0.50	-0.73	-0.30	-10.89	-1.13	-4.16	-1.58	-2.74	-1.28
CMCC-ESM2	-2.77	-1.65	1.01	-1.65	-0.52	0.04	6.03	-1.84	7.51	0.87	-1.16	0.65
GFDL-ESM4	-1.05	-0.09	-0.59	-0.31	0.86	-0.92	-2.37	-0.44	-0.08	-3.47	3.11	-1.49
EC-Earth3-Veg	-0.64	-0.70	2.20	-2.48	0.32	0.03	-0.38	-1.03	0.25	-1.63	1.75	0.28
MPI-ESM1-2-LR	1.13	-0.42	2.77	-1.85	1.39	-0.76	6.60	0.45	5.59	-3.06	4.18	-0.56
IPSL-CM6A-LR	1.96	-0.48	0.67	1.46	1.32	-1.01	0.50	-2.07	1.40	0.35	1.99	-1.16
CanESM5	1.87	1.71	-0.36	-0.05	-0.19	0.75	-0.84	3.77	-1.16	-2.28	-1.72	0.54
CNRM-ESM2-1	2.75	2.40	-0.93	0.45	0.11	0.72	-5.80	-0.60	-3.25	-0.63	-0.75	-0.58
CESM2	3.43	1.14	0.19	2.02	-0.86	0.95	8.25	2.72	0.17	4.73	-1.53	2.16
NorESM2-LM	4.13	1.14	0.57	1.68	-0.26	1.00	11.53	2.72	1.97	4.24	0.57	2.03
	Mid latitudes						High latitudes					
	NBP _{anom}	sCO ₂	sT	sSM	T	SM	NBP _{anom}	sCO ₂	sT	sSM	T	SM
ACCESS-ESM1-5	-3.78	-2.24	-1.27	0.16	-0.62	0.20	-5.69	-4.79	-1.32	1.54	0.69	-1.81
UKESM1-0-LL	-0.67	0.70	-0.16	-1.03	0.09	-0.27	2.89	-0.59	-1.36	2.58	0.94	1.32
CMCC-ESM2	-2.29	-1.32	-0.80	0.22	-0.56	0.18	-19.22	-2.05	-6.31	-10.22	0.71	-1.36
GFDL-ESM4	-2.38	-0.83	-0.71	-0.25	0.31	-0.90	4.22	2.17	-1.20	5.08	-1.86	0.03
EC-Earth3-Veg	0.07	-0.26	2.29	-1.18	0.04	-0.83	-2.65	-1.12	5.40	-6.87	-1.57	1.51
MPI-ESM1-2-LR	-0.40	-0.56	1.68	-0.27	0.35	-1.60	-5.03	-1.64	0.28	-3.28	-1.18	0.79
IPSL-CM6A-LR	0.35	0.02	-0.45	1.22	0.92	-1.36	8.08	1.19	1.87	3.94	1.03	0.03
CanESM5	1.43	1.14	-1.07	1.13	-0.05	0.28	7.56	-0.61	2.62	1.19	2.20	2.17
CNRM-ESM2-1	5.50	2.58	0.11	0.65	0.55	1.63	11.57	7.26	0.82	1.91	0.65	0.94
CESM2	0.92	0.38	0.55	-0.60	-0.63	1.23	0.62	0.09	-0.59	3.11	-0.19	-1.81
NorESM2-LM	1.25	0.38	-0.16	-0.04	-0.39	1.45	-2.37	0.09	-0.23	1.01	-1.42	-1.83

10

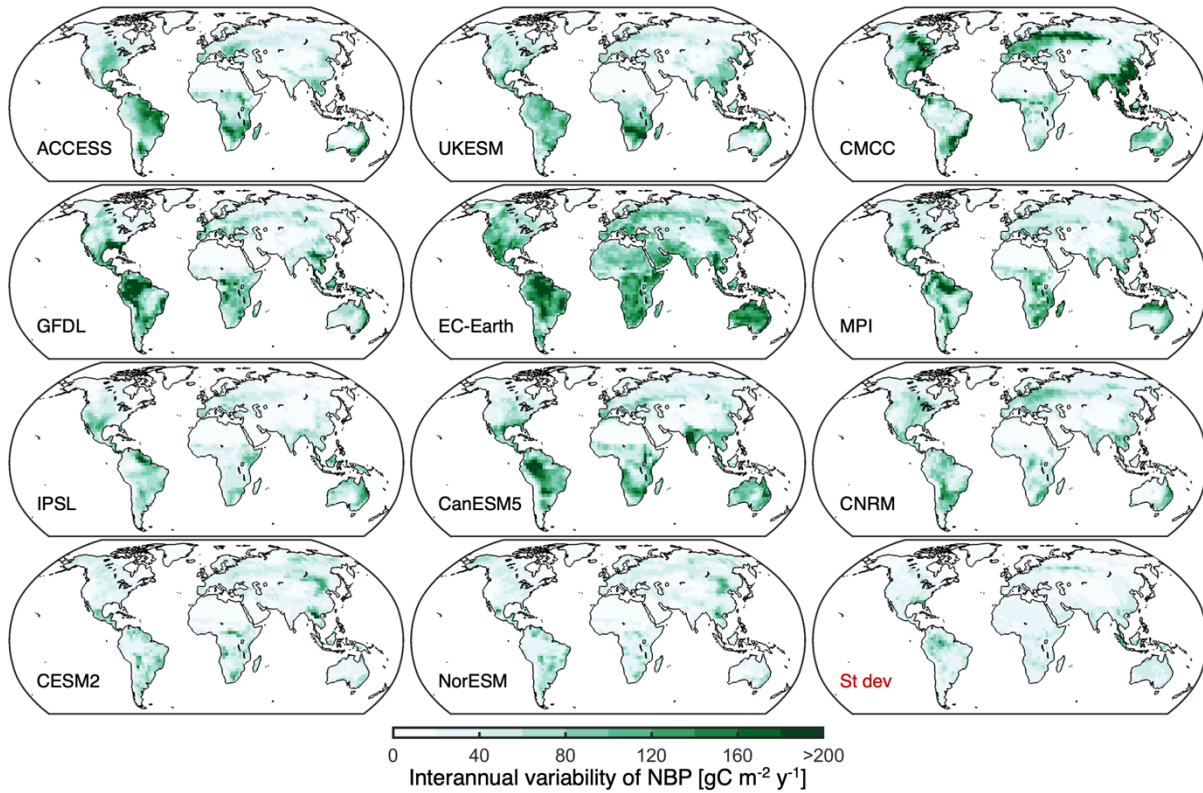
Table S3: Corresponding values from Fig. 7 showing contributions of the drivers to explain the anomaly in average projected NBP from individual models relative to the ensemble mean. The units of all values are gC m⁻² y⁻¹.



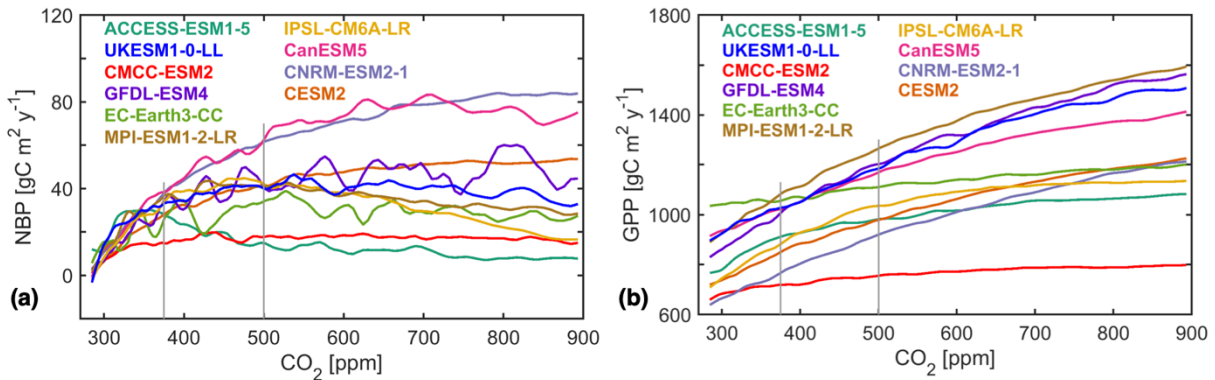
15 **Figure S1: Projected global land NBP from different Earth system models and different realizations of individual models for scenario SSP126.** The average value for each model is shown by the thicker lines, whereas thin lines represent single realizations. If a model does not have information over Greenland, NBP is set to zero. Cumulative global land NBP is estimated by multiplying the area-weighted average NBP times the land surface area excluding Antarctica ($135.22E6 \text{ km}^2$).



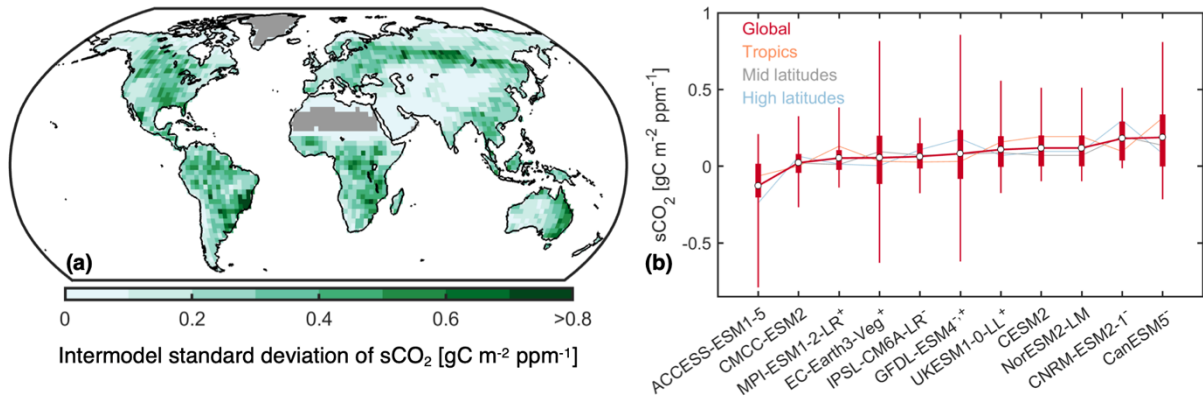
20 **Figure S2: Projected gross primary production (GPP), autotrophic respiration (RA), heterotrophic respiration (RH), and ecosystem disturbances (DIS) such as fires per Earth system model.** The global land cumulative fluxes from 2015 to 2100 are shown. The average value is shown for models with multiple realizations available. From left to right models are ordered according to increasing projected NBP. If a model does not have information over Greenland, fluxes are set to zero. Global land estimates are obtained by multiplying the area-weighted average flux times the land surface area excluding Antarctica ($135.22E6 \text{ km}^2$).



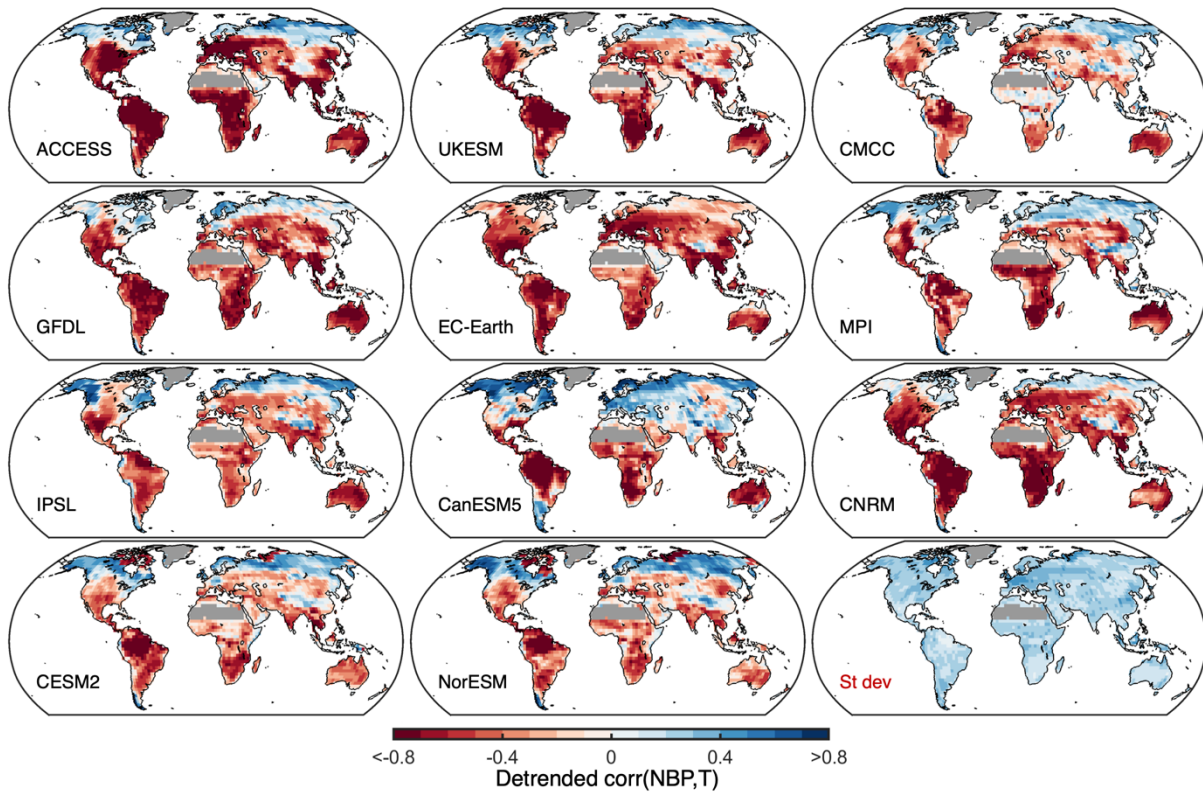
25 **Figure S3: Intermodel differences in interannual NBP variability.** Maps of the standard deviation from annual detrended projected NBP during 2015 to 2100 from individual models. The intermodel standard deviation is shown at the bottom right.



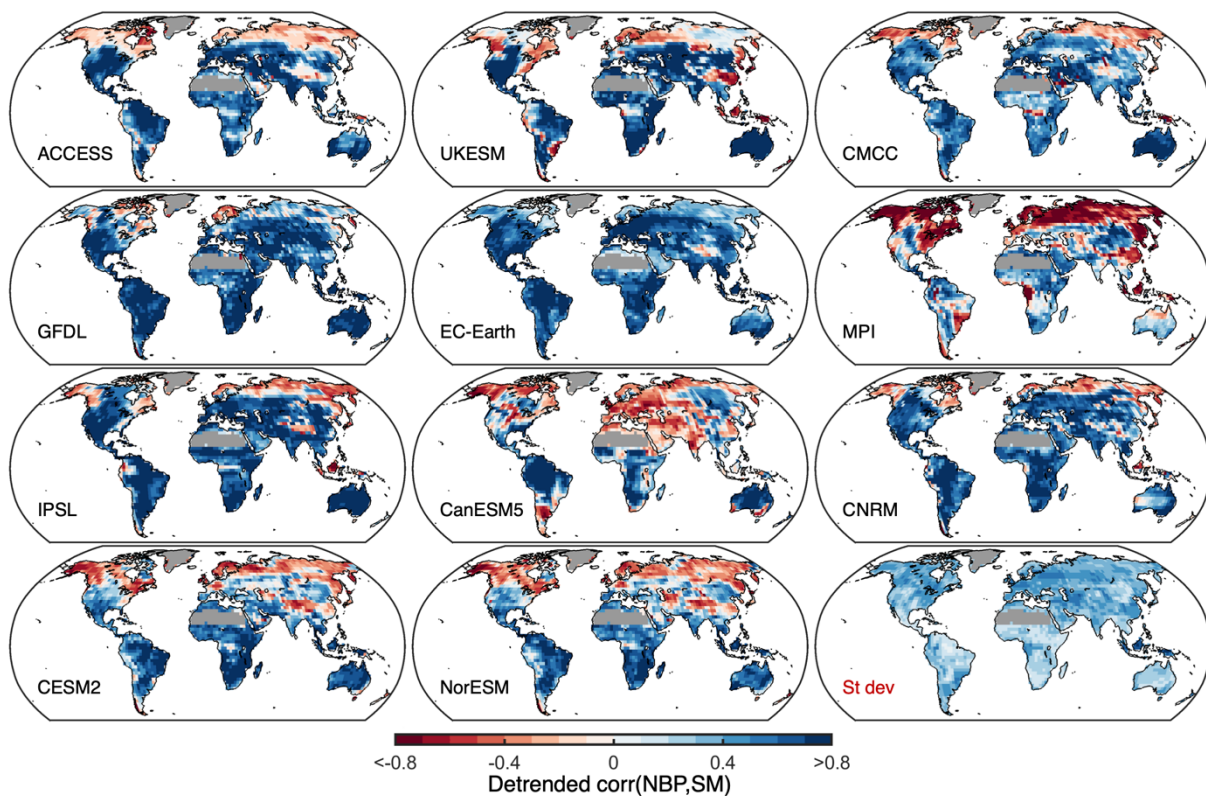
30 **Figure S4: Global land average NBP (a) and GPP (b) as a function of atmospheric CO₂ concentration for the 1pctCO₂-bgc simulations.** Smooth time series for NBP and GPP are obtained using a lowest fit with a 10-year window. Nevertheless, sCO₂ is computed as the slope of the linear regression for the unsmoothed annual data within the gray vertical lines where CO₂ concentration ranges from 375.8 ppm (year 29 of the simulation) to 501.5 ppm (year 58 of the simulation). If a model does not have information over Greenland, NBP and GPP are set to zero.



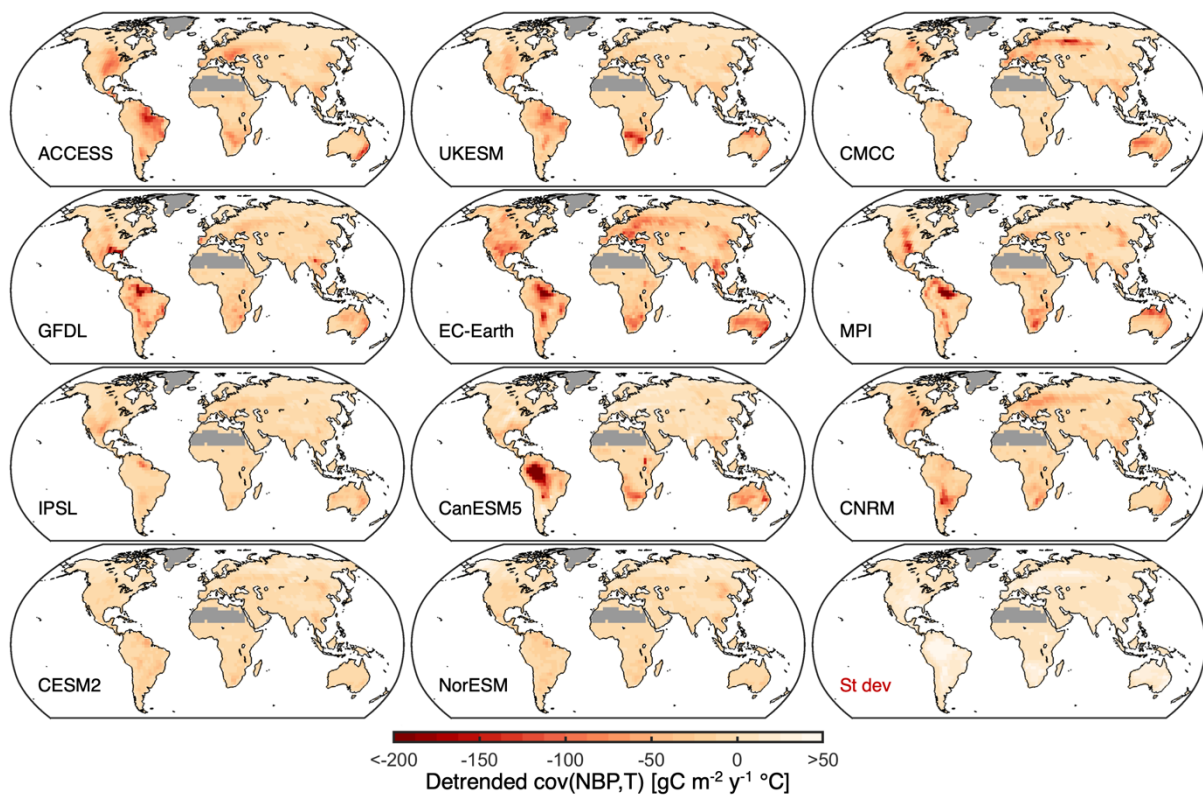
35 **Figure S5: Intermodel differences in the sensitivity of NBP to atmospheric CO_2 concentration ($s\text{CO}_2$).** (a) Intermodel standard deviation of $s\text{CO}_2$. (b) Distribution of $s\text{CO}_2$ from all land grid cells. The marker indicates the median $s\text{CO}_2$, the boxes span the interquartile range, and the whiskers span from the 5th to the 95th percentile. Additional lines indicate the median $s\text{CO}_2$ from land grid cells across the tropics, mid latitudes, and high latitudes. Models that do not include a nitrogen cycle are indicated by () and models that include dynamic vegetation are indicated by (+). Regions with 2015–2100 average GPP below $100 \text{ gC m}^2 \text{ y}^{-1}$ are masked in (a) and omitted in (b).



40 **Figure S6: Intermodel differences in the interannual correlation between detrended NBP and temperature.** The correlation is computed from the detrended time series of annual average NBP and annual average warm season T. In the extratropics (latitude $> 22.5^\circ$) the warm season is defined from March to October in the Northern Hemisphere and from September to April in the Southern Hemisphere, whereas in the tropics all months are considered. Regions with 2015–2100 average GPP below $100 \text{ gC m}^2 \text{ y}^{-1}$ are masked.



45 **Figure S7: Intermodel differences in the interannual correlation between detrended NBP and soil moisture.** The correlation is computed from the detrended time series of annual average NBP and annual average warm season SM. In the extratropics (latitude $> 22.5^\circ$) the warm season is defined from March to October in the Northern Hemisphere and from September to April in the Southern Hemisphere, whereas in the tropics all months are considered. Regions with 2015–2100 average GPP below $100 \text{ gC m}^{-2} \text{ y}^{-1}$ are masked.



50 Figure S8: Similar to Fig. S6 but for the covariance between detrended NBP and temperature.

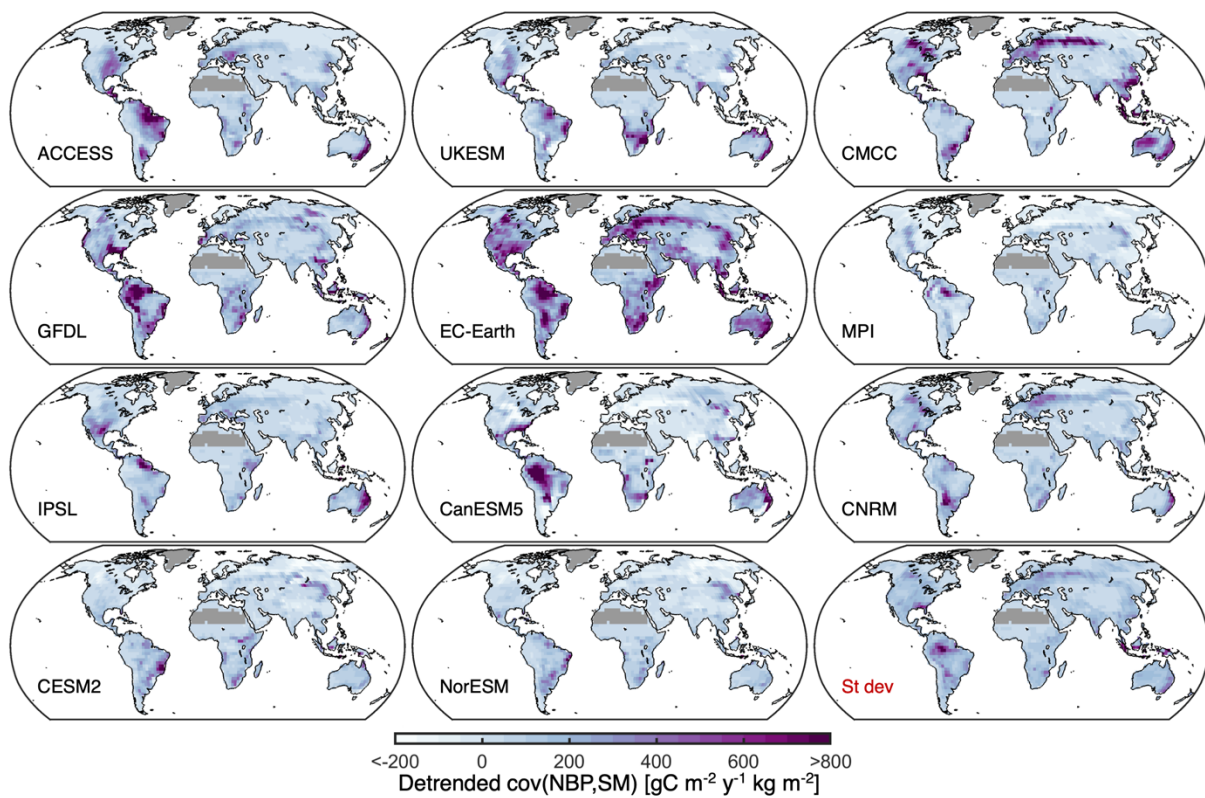


Figure S9: Similar to Fig. S7 but for the covariance between detrended NBP and soil moisture.

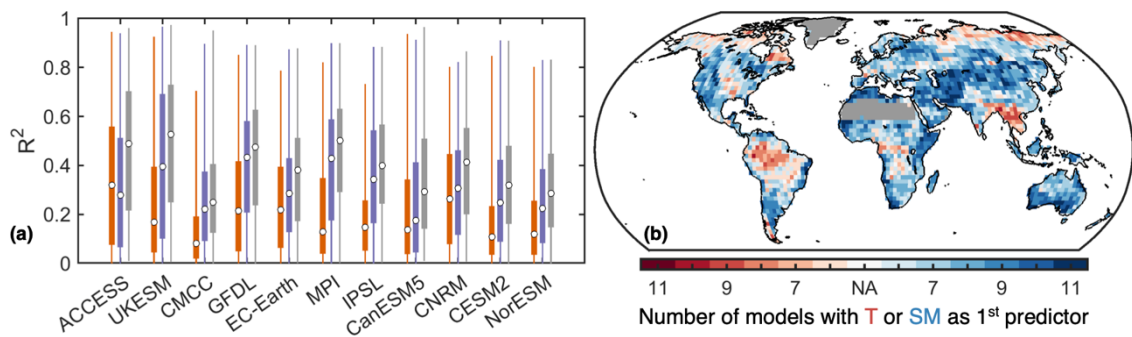
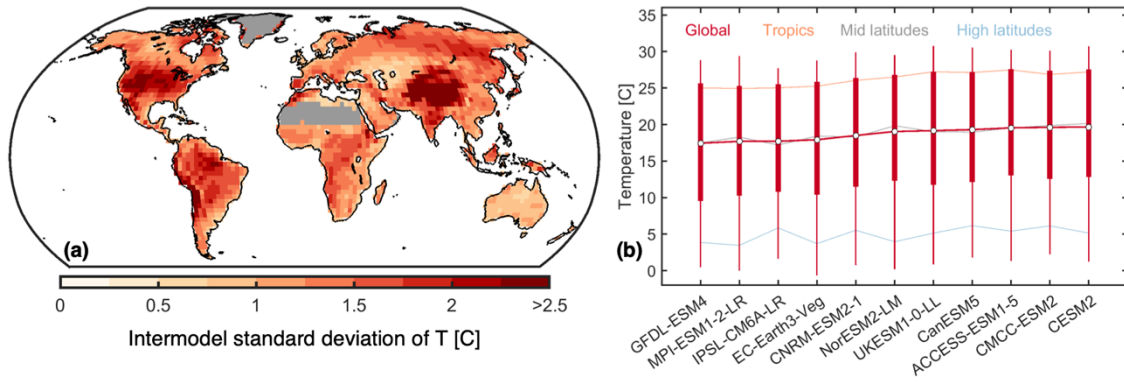
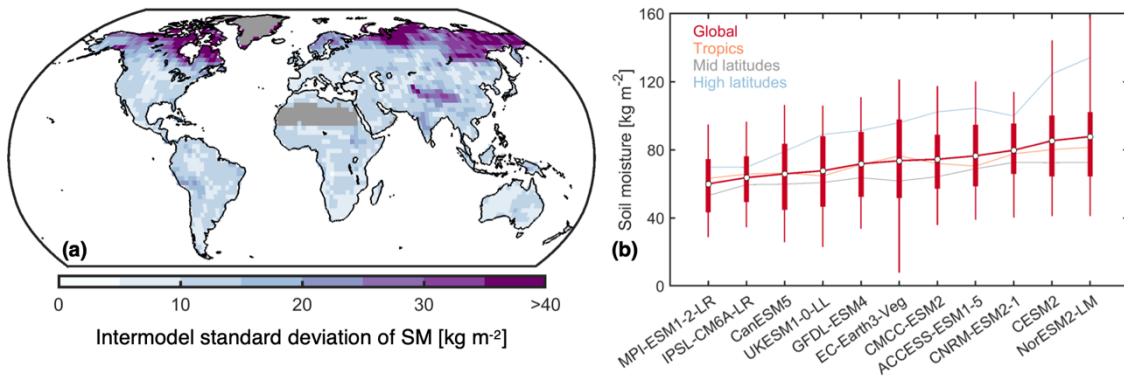


Figure S10: Similar to Fig. 4 but when considering soil moisture down to 1 m depth instead of the top 30 cm.



55

Figure S11: Intermodel differences in average warm-season temperature. (a) Intermodel standard deviation of long-term average T for the period 2015–2100. (b) Distribution of T from all land grid cells. The marker indicates the median T, the boxes span the interquartile range, and the whiskers span from the 5th to the 95th percentile. Additional lines indicate the median T from land grid cells across the tropics, mid latitudes, and high latitudes. Regions with 2015–2100 average GPP below 100 gC m² y⁻¹ are masked in (a) and omitted in (b).



60

Figure S12: Intermodel differences in average warm-season soil moisture. (a) Intermodel standard deviation of long-term average SM for the period 2015–2100. (b) Distribution of SM from all land grid cells. The marker indicates the median SM, the boxes span the interquartile range, and the whiskers span from the 5th to the 95th percentile. Additional lines indicate the median SM from land grid cells across the tropics, mid latitudes, and high latitudes. Regions with 2015–2100 average GPP below 100 gC m² y⁻¹ are masked in (a) and omitted in (b).

65

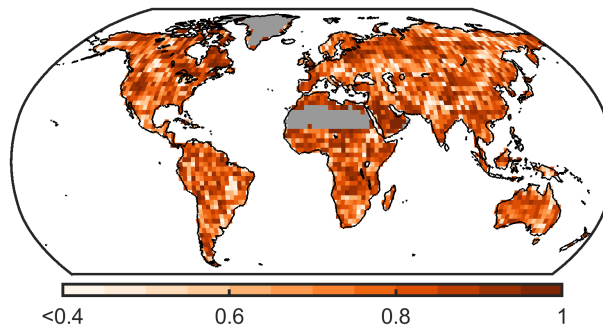
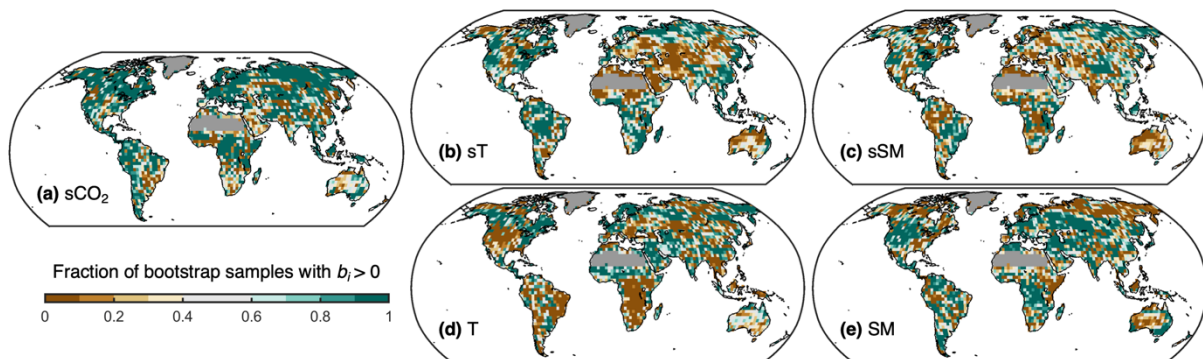


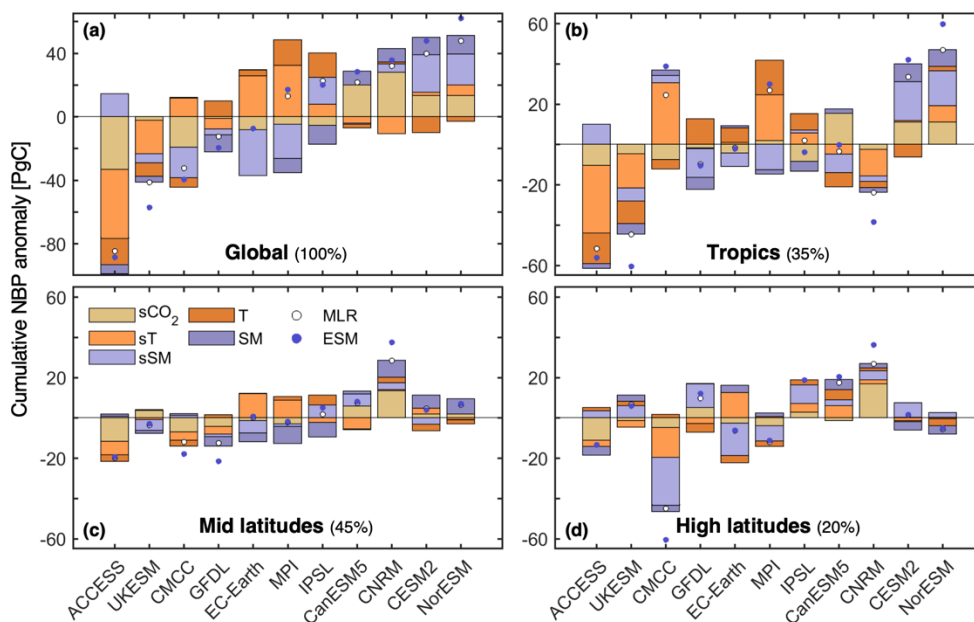
Figure S13: Pearson correlation between projected cumulative NBP from Earth system models and from the multiple linear regression. Cumulative NBP corresponds to the period 2015–2100. Regions with 2015–2100 average GPP below 100 gC m² y⁻¹ are masked.



70

Figure S14: Robustness of the influence of model characteristics on projected cumulative NBP. Fraction of 200 bootstrap samples with a positive regression coefficient b_i for (a) sensitivity to CO_2 concentration ($s\text{CO}_2$), (b) sensitivity to temperature (sT), (c) sensitivity to soil moisture (sSM), (d) long-term warm season average temperature (T), and (e) long-term warm season average soil moisture (SM). In this case the multiple linear regression at each grid cell is fitted considering only the covariance or only the correlation (whichever has the strongest absolute correlation with projected cumulative NBP) to represent sT and sSM . If both the correlation and the covariance are considered as in Eq. 1 of the article, then the signs of their corresponding regression coefficients b_i are less informative regarding the net effect of sT and sSM on cumulative NBP. Regions with 2015–2100 average GPP below $100 \text{ gC m}^2 \text{ y}^{-1}$ are masked.

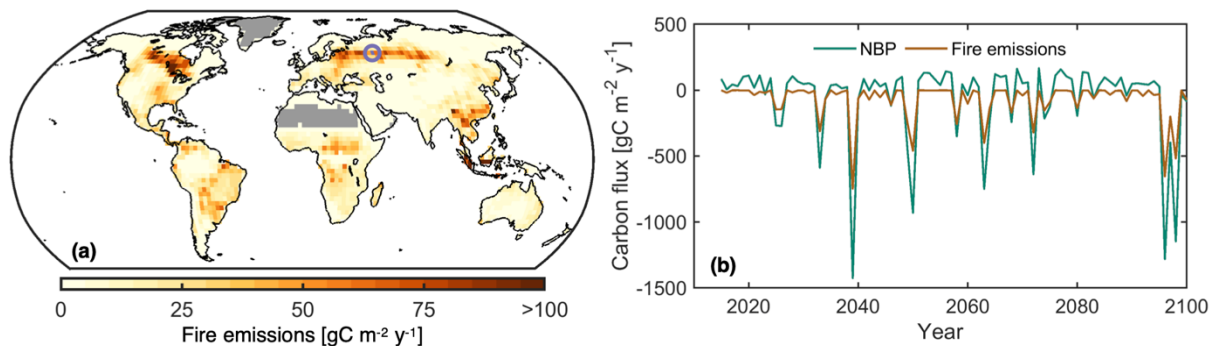
75



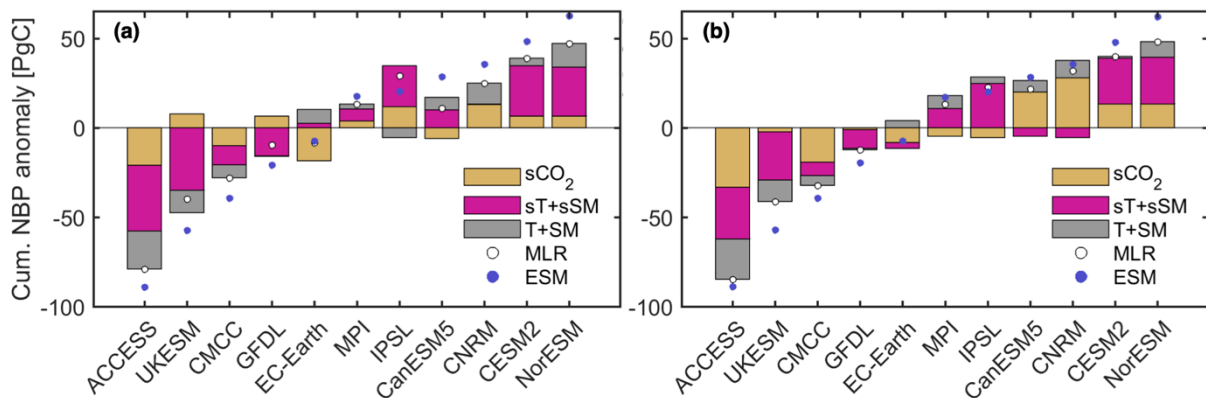
80

Figure S15: Contributions of the drivers to explain the anomaly in projected cumulative NBP from individual models relative to the ensemble mean. Bars indicate the contributions of the individual drivers estimated from the multiple linear regression. Dots indicate the total NBP anomaly based on the multiple linear regression (MLR) and from the actual model projections (ESM). All values correspond to averages from the 200 bootstrap samples. Results are shown for (a) global land, (b) the tropics ($22.5^\circ\text{S} - 22.5^\circ\text{N}$), (c) mid latitudes ($22.5^\circ\text{N} - 47.5^\circ\text{N}$ over North America, $22.5^\circ\text{N} - 55^\circ\text{N}$ over Europe and Asia, and $> 22.5^\circ\text{S}$), and (d) high latitudes ($> 47.5^\circ\text{N}$ over North America and $> 55^\circ\text{N}$ over Europe and Asia). The land percentage comprised in each region is noted next to the title: tropics represent 35.1% of the considered global land area, mid latitudes 44.8%, and high latitudes 20.1%. From left to right models are ordered according to actual increasing projected global land carbon sink.

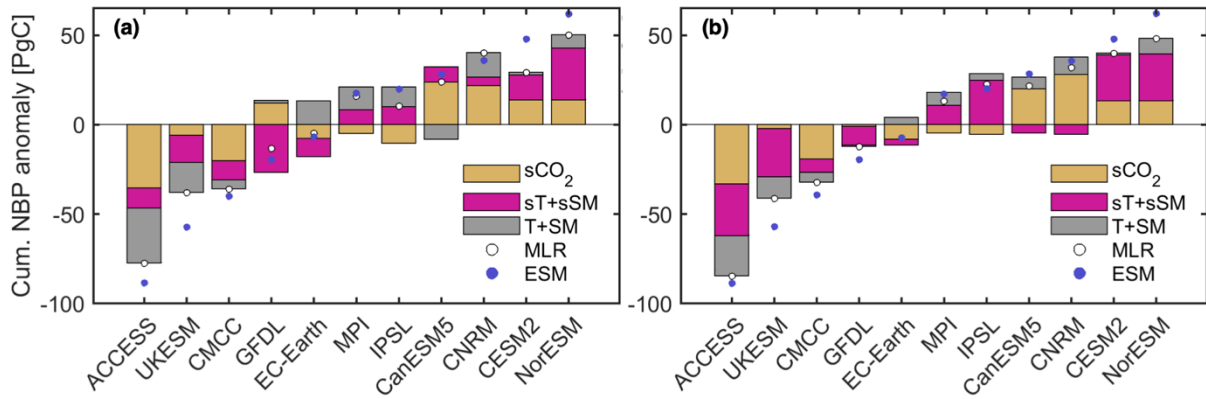
85



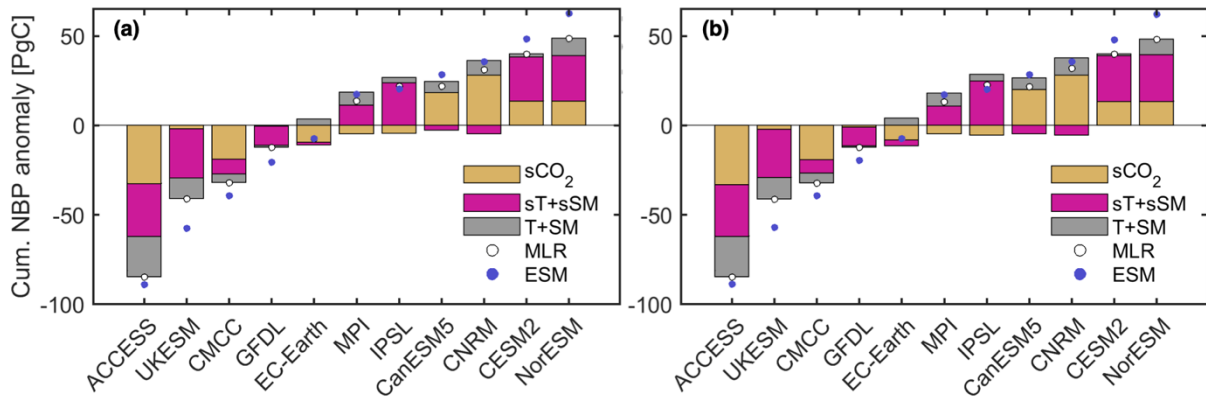
90 **Figure S16: Carbon fire emissions from the CMCC-ESM2 model.** (a) Long-term average fire emissions for the period 2015–2100. Regions with 2015–2100 average GPP below $100 \text{ gC m}^{-2} \text{ y}^{-1}$ are masked. (b) Temporal evolution of NBP and fire emissions for the high latitude boreal forest grid cell indicated in the map. A negative value indicates a carbon flux from land to the atmosphere.



95 **Figure S17: Comparison to Fig. 8 when changing the definition of $s\text{CO}_2$.** (a) Results when $s\text{CO}_2$ is defined as the sensitivity of GPP to rising CO_2 . (b) Same as Fig. 8. Bars indicate the grouped contributions of $s\text{CO}_2$, $s\text{T} + s\text{SM}$, and $\text{T} + \text{SM}$ to the NBP anomaly estimate from the multiple linear regression. Dots indicate the total NBP anomaly based on the multiple linear regression (MLR) and from the actual model projections (ESM). All values correspond to averages from the 200 bootstrap samples. Global land estimates are obtained by multiplying the area-weighted averages times the land surface area excluding Antarctica ($135.22\text{E}6 \text{ km}^2$). From left to right models are ordered according to actual increasing projected land carbon sink.



105 **Figure S18: Comparison to Fig. 8 when changing the definition of sT and sSM.** (a) Results when sT and sSM are estimated from the 1pctCO2-rad simulations. Here we use a time series of 30 annual values available in the simulations in which CO₂ concentration ranges from approximately 375 ppm to 500 ppm. In this case we also employ the detrended time series of annual mean NBP and detrended annual mean warm-season T and SM. The removed trends are computed using a lowess fit with a 10-year window. All models have only 1 realization for the 1pctCO2-rad simulations, except MPI-ESM1-2-LR which has 3. Also, EC-Earth3-CC is used as a substitute for EC-Earth3-Veg. (b) Same as Fig. 8. Bars indicate the grouped contributions of sCO₂, sT plus sSM, and T plus SM to the NBP anomaly estimate from the multiple linear regression. Dots indicate the total NBP anomaly based on the multiple linear regression (MLR) and from the actual model projections (ESM). From left to right models are ordered according to actual increasing projected land carbon sink.



110 **Figure S19: Comparison to Fig. 8 when changing the latitudinal threshold for computing annual mean warm season temperature and soil moisture in the estimation of sT and sSM.** (a) Results when setting the threshold at 30° instead of 22.5°. (b) Same as Fig. 8. Bars indicate the grouped contributions of sCO₂, sT plus sSM, and T plus SM to the NBP anomaly estimate from the multiple linear regression. Dots indicate the total NBP anomaly based on the multiple linear regression (MLR) and from the actual model projections (ESM). All values correspond to averages from the 200 bootstrap samples. Global land estimates are obtained by multiplying the area-weighted averages times the land surface area excluding Antarctica (135.22E6 km²). From left to right models are ordered according to actual increasing projected land carbon sink.

115